

Design Aspects for 5G V2X Physical Layer

Mate Boban, Konstantinos Manolakis, Mohamed Ibrahim, Samer Bazzi, Wen Xu
Huawei Technologies, German Research Center, 80992 Munich, Germany
Email: mate.boban@huawei.com

Abstract—Next generation 5G communication systems will need to employ a range of diverse technologies in order to support vehicle-to-everything (V2X) use cases, ultimately leading to accident-free, cooperative autonomous vehicles that use the available roadway efficiently. V2X is considered as one of the most challenging applications of 5G, as it requires ultra-reliable and low-latency communication for safety-critical use cases and has to provide high data rates in many scenarios. This paper discusses design aspects for the radio access in 5G V2X. Selected key technologies and their integration towards future 5G V2X physical layer are addressed. We discuss channel modeling in the context of 5G V2X use cases and we present first results for frame structure and numerology design, coexistence with earlier systems, multi-link synchronization, and multi-antenna transmission techniques.

I. INTRODUCTION

During the last years, mobility and vehicular transportation is developing rapidly. New societal trends affecting the transportation are urbanization, stringent emission- and energy-related regulations, and the need for more efficient public transport systems. On the other hand, key market trends include the advent of automated driving, new modes of vehicle usage and ownership (e.g., car and ride sharing). These trends create a shift towards more reactive and intelligent transportation systems.

V2X communication will play an important role in reaching these goals. V2X is considered as an important component of fifth generation (5G) networks, which aims to satisfy high demands in terms of data rates, latency, reliability and number of connected devices. As explained in [1], the general goal is to deliver 1000 times more data throughput, serve 10 to 100 times more devices and reduce the minimum latency by a factor of 5, compared to the existing 3rd Generation Partnership Project (3GPP) Long Term Evolution (LTE) networks.

This paper discusses the role of existing communication systems in 5G V2X and proposes enhancements on key aspects of the physical layer. We first discuss V2X channel modeling as the key aspect for realistic evaluation of 5G V2X systems. In order to meet latency, reliability and throughput requirements, multi-link synchronization, frame structure design, and multi-antenna transmission are discussed as key enabling technologies on the physical layer. For each of the technologies, we present preliminary results and discuss the necessary future work.

The rest of the paper is organized as follows. Section II describes different communication systems for enabling V2X. Section III describes the most important V2X requirements in light of 5G network design goals, based on which key technologies are proposed for the 5G V2X physical layer. Finally, conclusions are discussed in Section IV.

This work has partly been performed in the framework of the Horizon 2020 project FANTASTIC-5G (ICT-671660) receiving funds from the European Union. The authors would like to acknowledge the contributions of their colleagues in the project, although the views expressed in this contribution are those of the authors and do not necessarily represent the project.

II. V2X COMMUNICATION SYSTEMS

Figure 1 shows the proposed architecture for providing V2X services in the future 5G network. V2X services can be supported by several communication sub-systems, which need to be integrated into a new 5G architecture to meet the V2X requirements. While this paper focuses on physical layer technologies for radio access, we note that, beyond the radio access communications systems, the network architecture supporting V2X would benefit from concepts such as: i) Mobile Edge Computing (MEC), wherein delay-critical functionalities are moved closer to the network edge (Fig. 1); ii) different functionalities in the core network such as access to traffic information system, automotive OEM-specific functionalities (e.g., servers running proprietary use cases), and teleoperation centers for remote control of the vehicles.

This section briefly describes the communication system components and discusses how these can be further extended and integrated.

A. Cellular Network

Elaborating on the modes described in [2], we consider that future cellular systems will be able to support V2X communication through three distinct modes, as shown in Fig. 1: *Cellular V2X*, *Cellular-assisted V2V* and *Cellular Ad Hoc V2V*.

Cellular V2X refers to “classic” cellular communication, wherein a vehicle equipped with a user equipment (UE) is directly communicating with a base station to reach either a server or to connect to another vehicle. Apart from macro cells, the scenario also includes small cells, mainly in the form of Road Side Units (RSUs), as shown in the bottom left of Fig. 1, to improve coverage and the overall cell throughput, but also to allow them having enhanced functionalities compared to IEEE 802.11p stations. Such can be fast initial radio access and handover between RSUs and coordinated low-latency scheduling and resource allocation.

Cellular-assisted V2V is a scheme where the base station coordinates the V2V communication between nearby vehicles by instructing them on which resources to use and for how long, which vehicles to communicate with (e.g. managing priority in case of different V2V applications competing for resources [3]). This mode is best suited for extremely low latency, high reliability V2V communication, as the base station makes sure that the resources are available when needed and time-consuming data transmission over the base station is avoided.

Cellular Ad Hoc V2V is a mode where vehicles communicate directly, without assistance from the base station. Since it does not involve the base station, it has some similarities with IEEE 802.11p and can be used for safety-relevant information exchange in cases with no cellular coverage. Main enhancements of cellular ad hoc V2V compared to IEEE 802.11p lie in the spectrum usage and the initial access procedure. A subset of the cellular frequency

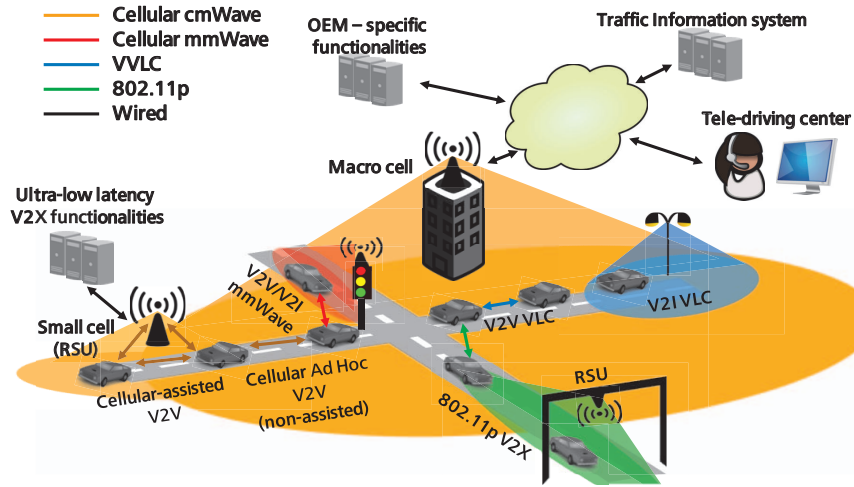


Fig. 1. Heterogeneous multi-radio V2X network, which includes cellular systems in centimeter (cmWave) and millimeter (mmWave) frequency bands, IEEE 802.11p, and vehicular visible light communication (VVLC).

band can be reused in areas without or with partial cellular coverage for communication between vehicles. In a general sense, resource usage can be considered to be under tacit control of the cellular network (i.e., the network determines which resources vehicles can use), thus simplifying a re-transition back to cellular V2X. Moreover, out-of-coverage users can remain time-synchronized to the cellular network in order to communicate with in-coverage users, allow for interference-free multi-link connectivity of the latter ones, and quickly attach to a base station if again in coverage.

1) *Millimeter-wave for V2X*: Riding on the trend of reduced cell sizes in search for increased network capacity and the need for more available spectrum, millimeter wave (mmWave) band has seen a resurgent research interest [4], [5]. The authors' vision for the role of mmWave in V2X is twofold:

- 1) Directional V2V communication for supporting particular V2X use cases, such as back-to-front communication between subsequent vehicles.
- 2) V2I communication, wherein short-lived, high data rate connection can be established between vehicle and nearby base station to exchange delay-insensitive data.

Although mmWave communication is very attractive for high data rates, it faces challenges on the physical layer. Due to its susceptibility to shadowing, it is deemed suitable for mostly short range (a few hundred meters) and point-to-point LOS communication [6]. Furthermore, since the Doppler spread is linear in the carrier frequency, in the 60 GHz band it will be ten to thirty times that of in 2-6 GHz band. This calls for a special frame design and numerology for mmWave.

B. IEEE 802.11p

The incentive for using the IEEE 802.11p protocol suite stems from U.S. and European regulators reserving 75 MHz and 30 MHz bands respectively in the 5.9 GHz frequency range for ITS use. Some vehicle manufacturers announced proactive deployment of V2X systems based on IEEE 802.11p radios in the year 2016. IEEE 802.11p has been envisioned to support facilities provided related to cooperative awareness functionality (e.g., in Europe, through Cooperative Awareness Messages –

CAMs [7]) and event-based emergency updates for hazardous situations (e.g., through Decentralized Environmental Notification Message – DENM). IEEE 802.11p has a physical layer robust to Doppler spread and enabling low-latency communication thanks to its short radio frame. However, it suffers from high collision probabilities under medium/high loads due to its random access scheme, making it unsuitable for ultra-reliable communication.

C. System Integration Towards 5G V2X

Since telecom operators have been working on previous iterations of the system for decades, an LTE-based cellular system (as described in [2]) is likely to be the initial step towards 5G V2X in some markets. Similarly, due to the potential government mandates on the use of the technology and proactive approach of vehicle manufacturers, IEEE 802.11p-based systems will likely be deployed as the initial V2X technology in other markets.

In later phases, a new cellular system (e.g., based on new air interface in both cmWave and mmWave, as specified in Release 15 and beyond 3GPP specifications ¹) and other technologies shown in Fig. 1 shall play a role in 5G V2X. In terms of cmWave, new cellular radio interface currently specified is promising orders of magnitude higher reliability and lower latency, which is necessary to enable 5G V2X use cases. Furthermore, due to their beneficial characteristics in terms of increased bandwidth, strong directionality/low interference, and ability to support network densification, mmWave [5] and vehicular visible light communication (VVLC) [8] are candidate 5G V2X radio access technologies to support specific V2X use cases. These and possibly further technologies will be part of a more advanced 5G V2X system, bringing up an important design goal for 5G: the capability to support diverse technologies and forward compatibility.

III. 5G KEY TECHNOLOGIES FOR ENABLING V2X

The nature of V2X use cases is such that a challenging combination of low latency and high reliability, along with high data rates in some cases, is required. In order to support cooperative automated driving, cooperative intersection control, and safety

¹<http://www.3gpp.org/specifications/67-releases>

critical applications the network will need to support both very high reliability (above 99%) and low end-to-end latency (below 10 ms) [3]. While those requirements are shared with other 5G use cases, the inherent high mobility and diversity of vehicular environments make these requirements particularly challenging to fulfill for V2X. For example, achieving low latency for real time map update for automated driving might require placing certain functionalities close to the network edge (i.e., close to the actual roads to which the maps refer), since locating these functionalities in the core network might result in delays that are too high to provide timely update. Next, we describe how these seemingly contradictory requirements can be satisfied concurrently.

Achieving low latency: Enabling low latency in V2X does not differ significantly from other latency-stringent applications. However, there are some particularities that need to be taken into consideration when designing a communication system capable of achieving low latency in a V2X setting. End-to-end latency requirements for V2X use cases can vary significantly, ranging from seconds (e.g., in case of Traffic Flow Optimization or Automated Parking System [9] use case), to under one hundred milliseconds (cooperative message exchange [7]), to under ten milliseconds (e.g., Cooperative Collision Avoidance (CoCA) of connected automated vehicles [3]). Therefore, the network management needs to be flexible enough to provide latency requirements without sacrificing efficient resource use. Key technologies on the physical layer for low and flexible latency requirements are a new frame structure and fast initial access.

Achieving high reliability: Reliability is of paramount importance for a large number of V2X use cases, particularly those related to safety (e.g., Cooperative Collision Avoidance (CoCA) of connected automated vehicles, Teleoperated Support (TeSo), etc. [3]). In order to achieve high reliability on the physical layer, numerology adjusted to the V2X channel, channel coding for error floor, feasible rate matching and ARQ, along with multi-antenna transmission techniques are necessary.

Achieving high throughput: Reaching this goal needs multiple-antenna beamforming techniques in order to mitigate interference and potentially transmit more data streams. Furthermore, additional spectrum will be needed, which will be most probably found in the mmWave frequency bands.

A. Channel modeling

The first step towards a proper design of the physical layer is the deep understanding of the V2X channel model. To design a 5G V2X system that provides ultra high reliability required for the challenging use-cases (e.g., Information sharing for full automated platooning, Intersection Safety Information Provisioning for Urban Driving [3], etc.), existing channel models need to be further extended, as the existing models were either developed for specific frequency (e.g., 5.9 GHz), with low-speed vehicle movement, or for V2I communication only (e.g., [10]). Furthermore, newly developed channel models for 5G systems described in [11] do not fully support dual mobility, which is necessary for V2V communication because of strong scattering and high mobility on both sides of the link resulting in more dynamic channels.

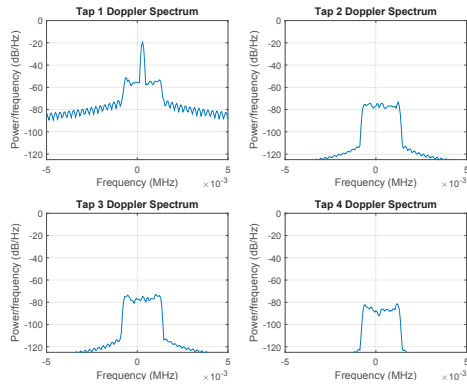
In terms of the V2X channel generation process, we can distinguish four main steps: 1) Selecting the link type (e.g., V2V, V2I, V2P, etc.) and scenario (e.g., highway, urban, rural); 2) Assigning propagation condition to the link (i.e., LOS or non-LOS); 3) Calculating path loss and shadowing; and 4) Calculating

small scale parameters (path delays, arrival and departure angles, etc.).

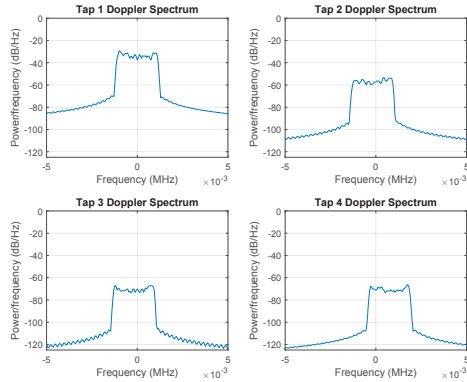
While the first step is trivial, the second step – assigning realistic propagation condition to V2X links – is important because of: i) high mobility, potentially on both sides of the link, which creates dynamic LOS blockage patterns and ii) low antenna heights resulting in frequent blockage. Realistic LOS blockage and its evolution was investigated for V2V channels in [12]. Realistic vehicular mobility and building locations were taken from maps and analysis of the LOS probabilities in real cities and on highways was done for different traffic densities. In order to model the time evolution of LOS blockage for V2V links, a three-state discrete-time Markov chain was used, comprised of LOS, non-LOS due to static objects (e.g., buildings, trees, etc.) and non-LOS due to mobile objects (vehicles). Results presented in [12] showed significant difference compared to standard cellular models for LOS blockage, thus emphasizing the need for bespoke modeling of blockage for V2X links.

The third step – calculating path loss and shadowing – has also been studied extensively for V2X channels. Karedal et al. [13] analyzed the path loss in different environments (rural, urban, suburban) and showed varying path loss exponents apply for different environments and link types. In terms of characterizing shadow fading, Meireles et al. [14] performed V2V measurements and showed that a single vehicle can incur more than 10 dB attenuation. Further measurement-based studies have developed models for vehicular shadowing in either geometry based deterministic [15] or geometry based stochastic [16] manner.

In terms of the final step – calculating small scale parameters – channel models need to capture the delay and Doppler spread, fading statistics, and non-stationarity. Three main types of small scale channel models are: tap-delay, geometry-based stochastic, and ray-based models. In tap-delay models, the impulse response of the channel is modeled with components at certain delays (“taps”). While the average power per-tap power is often assumed to decay exponentially with delay, the fading is implemented by varying the amplitude of each tap over time according to specified distributions. The channel can be modeled with a strong LOS path (e.g., Fig. 2(a)), or without LOS (Fig. 2(b)). Each tap may feature individual Doppler spectrum, which for vehicular channels was shown to be of complex shape (as shown in Fig. 2). Fig. 2 also shows how the large scale propagation condition (i.e., being in LOS or non-LOS state) affects the small scale fading. In general, statistics of vehicular channels may change over time, because many of the scattering clusters (vehicles) are mobile and as the distance between transmitter and receiver and reflectors changes. The non-stationarity cannot be captured by tap-delay models, therefore either geometry-based stochastic [17] or ray-based models [18] need to be employed. Geometry-based stochastic models use a map of the surroundings (either real or abstracted, such as a rectangular grid for a city) to randomly generate scatterers based on distributions that can be extracted from measurements. On the other hand, ray-based model, in addition to using detailed map of the surroundings, use ray shooting and geometry-based deterministic calculations of paths they take as they interact with the surroundings to generate the channel at the receiver. Many of the specific characteristics of vehicular channels discussed above are not captured in existing standard models and therefore require additional study.



(a) Highway same direction LOS Channel.



(b) Highway same direction non-LOS Channel.

Fig. 2. Doppler spectrum per channel tap of exemplary V2V channels. Channel structure (Doppler shapes and tap structure) are generated based on the results from Acosta-Marum and Ingram [19] at 5.9 GHz and speeds of approximately 100 km/h.

B. Coexistence and multi-link synchronization

One of the challenges which 5G V2X will have to deal with is the coexistence of different technologies, especially in the early phase of 5G. It is expected that 5G will coexist with earlier systems such as evolutions of LTE and other systems, as described in Section II. In case of distanced frequency spectra, such as cmWave and mmWave bands, dedicated radio interfaces, transceivers and most probably protocol stacks will be used. However, it is foreseen that within a single frequency band, parts of the spectrum will be shared or even reused between more than one (sub-)system or radio links. Supporting so-called multi-connectivity, or even maintaining multiple radio links within a single band is not only a practical implementation choice for the transition towards 5G, but offers benefits of flexible frequency usage and – especially for mmWaves – enhanced link robustness for ultra-reliable communication.

Interference-free coexistence between multiple radio links needs careful design. As an example, cellular V2V may be located in the same frequency band with existing cellular links. Unlike using a dedicated band, so-called in-band V2V comes with additional requirements. Even if orthogonal resources are used between V2V and cellular links, interference-free coexistence needs accurate time synchronization between multiple links, as the usage of additional overhead for frequency guard bands should be avoided. Synchronization must still be maintained between multiple V2V links of the same or different users, even if an active link to the base station is not provided.

Advanced synchronization schemes must provide solutions for

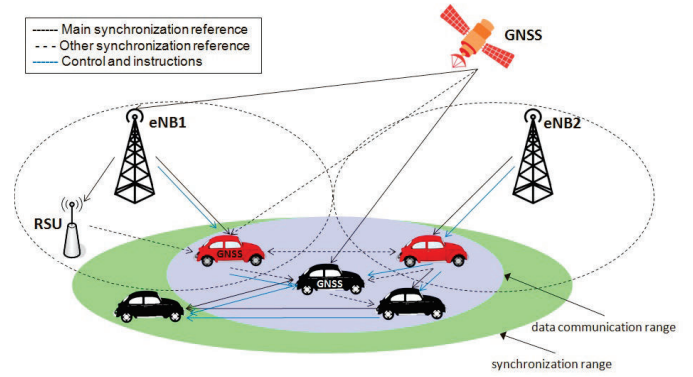


Fig. 3. Scenario with in- (red) and out-of-coverage (black) users; base stations and users may be equipped with a GNSS receiver. Priorities in synchronization source selection are combined with control and instructions provided by the base stations and forwarded to out-of-coverage users. In downlink and sidelink, dedicated synchronization signals are sent.

inter-cellular V2V, as shown in the general scenario by Fig. 3, also with potentially non-synchronized base stations. Vehicular networks with partial or even no cellular coverage need to be considered as well. Multiple synchronization sources, including base stations, RSUs, Global Navigation Satellite System (GNSS) and mobile users are available and need to be hierarchically prioritized, whereas the overall control remains on the cellular network side, as proposed by the authors in [20]. Key solution aspects include the assignment of a sidelink-aware timing advance index to each sidelink-capable user, so that the transmissions of all users are aligned and multiple sidelink and cellular (most probably uplink) signals reach the intended receivers within the duration of the guard period. As some users may be driven by different external synchronization sources, the time offset of the base station with respect to a globally agreed reference must be transmitted to the users, together with control and other synchronization-relevant information. According to the solution, while in-coverage users prioritize their serving base station, out-of-coverage users rely on GNSS or other in-coverage users for their own synchronization, following the instructions given by the base station, which are forwarded to them through in-coverage attached users. In the most challenging scenario with inter-cellular V2V and non-synchronized base stations, the options of temporarily disconnecting the cellular link sharing a band with the sidelink, or even handing over cell-edge users between adjacent base stations, needs to be considered by the cellular network.

For partial and out-of-coverage scenarios, an iterative algorithm can be used for mutual users' time synchronization, as described in [20]. Through the sidelink, users exchange predefined synchronization signals as in downlink, similar to 3GPP signals described in [21]. These signals are detected by other sidelink users, which adjust their time reference according to a weighted mean of the timing of other users. After a few iterations all users converge to the same time reference. Here, performance is evaluated for two exemplary scenarios: an out-of-coverage scenario and a partial coverage scenario in which some users are equipped with a GNSS receiver. According to the method, only out-of-coverage users without GNSS update their own time reference, based on received sidelink synchronization signals, which are weighted differently according to synchronization source type. Time references obtained by GNSS, sidelink signals from in- and

from out-of-coverage users are weighted with a relative ratio of 10:5:1. It is assumed that synchronization signals are transmitted from all users during one update cycle, allowing them to update their timing in every iteration. For a more detailed description of the algorithm the authors refer to [20].

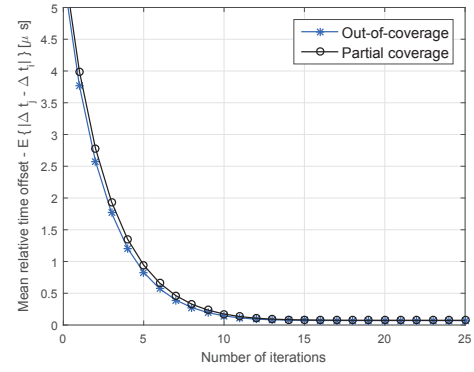
Fig. 4(a) shows the *relative* time offset between users mutually synchronizing, whereas Fig. 4(b) shows their *absolute* time offset w.r.t. the network reference. In the considered example, 20 users are uniformly distributed within a circle of 100 m radius. In the first setting, all users are considered to be out of coverage without access to any external synchronization source, while in the second partial coverage setting 5 users are assumed to be in cellular coverage and 5 more out-of-coverage users to have a GNSS receiver.

The time errors are modeled as Gaussian-distributed random variables with zero mean and a Root Mean Squared (RMS) value of 60 ns for the base station, 10 ns for GNSS and an 5 μs (initial error) for the mobile users. On the receiver side, an estimation error with RMS of 100 ns is assumed for downlink and sidelink signal detection. As observed in Fig. 4, when some users are in cellular coverage and some out-of-coverage users are equipped with GNSS, results are comparable in terms of the relative time error, with a residual error below $0.2\mu\text{s}$. In the out-of-coverage scenario, where no external reference is available, the synchronization error estimation is subject to a time drift, as the algorithm aims to compensate the wave propagation times. However, for networks with partial coverage, where some users follows their own fixed reference, the *absolute* time error is the most relevant performance indicator. And as shown, for the absolute time error of out-of-coverage users the drift disappears and the residual error floor increases only a little compared to their relative error. The residual error, which was here found to be $0.3\mu\text{s}$, will depend on the accuracy of the synchronization sources, the receiver-side estimation errors and the radio wave propagation times according to the distances.

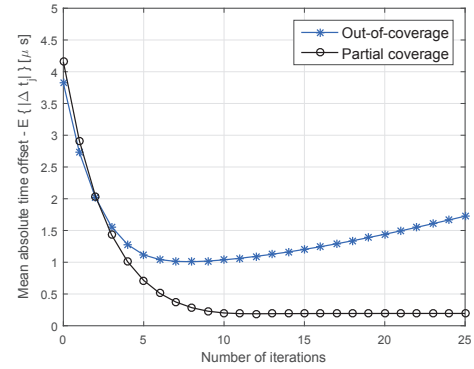
C. Numerology and frame structure

One of the contributions to the end-to-end latency comes from the physical layer, with the Transmission Time Interval (TTI) being the main contributor. LTE deploys a rigid frame structure with a fixed TTI of 1 ms. To meet the strict latency requirements of V2X, the TTI may be flexibly shortened, following two main approaches: reducing the symbol duration by increasing the subcarrier spacing (5G approach, see also the self-contained frame structure [22]), or fixing the subcarrier spacing and reducing the number of symbols per frame (LTE/4G approach, the symbol-wise frame structure).

Fig. 5 shows the frame structure for both approaches. The figure also shows the drop in theoretical capacity of the wireless link over the Doppler shift for different SNR values and a fixed channel RMS delay of $0.1\mu\text{s}$. In the considered example, the latency constraint is $250\mu\text{s}$. The symbol-wise frame structure spans 3 OFDM symbols, whereas the subcarrier spacing of the self-contained frame structure is tuned to 60 KHz, a cyclic prefix of $1\mu\text{s}$, a guard period of $20.33\mu\text{s}$ and allocating 12 symbols for downlink and 1 symbol for uplink. This numerology is chosen as a rough scaling of a factor 4 of the LTE numerology as agreed in [23]. Fixing the subcarrier spacing to 15KHz as in LTE has the advantage of coexistence and backwards compatibility. Here, the capacity is computed taking into consideration the nominal



(a) Relative error.



(b) Absolute error.

Fig. 4. Relative (a) and absolute (b) time error w.r.t the ideal reference for out-of-coverage and partial coverage network scenarios with 20 users. In partial coverage, 5 users are in cellular coverage and 5 more users have a GNSS receiver.

SNR and the Minimum Mean Squared Error (MMSE) of channel estimation considering Wiener filtering. The self-contained frame structure utilizes a preamble pilot pattern where one symbol is dedicated for training, whereas the symbol-wise frame structure has a scattered pilot pattern.

As can be observed in Fig. 5, in the high SNR regime the 5G frame structure achieves a higher capacity up to a certain Doppler shift, beyond which the symbol-wise frame structure becomes more robust towards the Doppler shift. This is a result of the different pilot patterns of the self-contained and symbol-wise frame structures. Preamble-based design is not suitable for highly time-variant channels since the channel knowledge may become outdated. For more details on the comparison of the frame structures, we refer the reader to [24]. The self-contained frame structure offers other advantages: using Time Division Multiplexing (TDM) for pilot, control and data facilitates the decoder's processing, compared to a scattered pilot pattern where the receiver needs to wait until the end of the frame before performing channel estimation. Moreover, the self-contained frame allows for faster feedback within the same frame, compared to the symbol-wise frame structure. Having a flexible numerology as in the self-contained frame structure, offers an additional degree of freedom to adapt PHY layer transmission to various service requirements and channel conditions. However, in order to overcome the performance degradation during the fast fading V2X channels, additional scattered pilots should be multiplexed in the data segment in order to mitigate channel estimation errors due to the expiration of the channel knowledge.

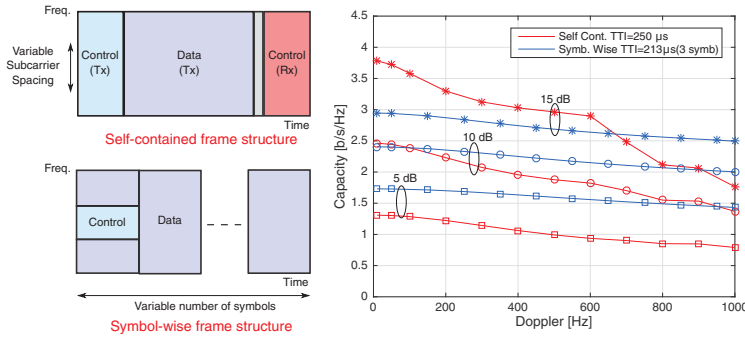


Fig. 5. Low latency flexible frame structures based on 5G and LTE numerologies (left) and their theoretical achievable capacity vs Doppler for different SNR (right).

D. Multi-antenna techniques

In addition to different antennas needed to support multiple communication technologies described in Section II, relatively large dimensions of vehicles allow for placement of additional antennas. Due to the geometry of vehicular traffic, where vehicles travel in delineated lanes, having multiple antennas placed at different locations (e.g., the corners of a vehicle) can contribute so that shadowing caused by other vehicles in V2V communication is alleviated or even mitigated. Furthermore, such antenna placement results in less correlated channels, which is a favorable property for MIMO techniques.

The main goal of multi-antenna transmission in V2X is to enhance reliability by using the available degrees of freedom for either increasing diversity or mitigating interference; in both cases, the users' signal-to-interference-plus-noise ratio (SINR) will be increased. Achieving higher data rates through spatial multiplexing techniques is a secondary goal and relevant for high-throughput V2X use cases. Spatial diversity is the main diversity source in V2X, as time diversity is naturally constrained by low-latency requirements and frequency diversity gains are expected to be limited by the available bandwidth. Therefore, robust data precoding can be used to ensure that reliable multi-link communication can be established, while on the receiver side multiple antennas shall further increase the SINR through combined signal reception and interference cancellation.

To illustrate the theoretical MIMO gains within the V2V context, we investigate the relationship between the number of antennas per vehicle N and the SINR of a target vehicle in a three lane scenario as shown in Fig. 6. Here, the target vehicle receives a signal from a desired vehicle and is affected by interference coming from six neighboring vehicles. The distances between the cars in each lane are modeled as exponentially distributed with parameter λ chosen based on medium traffic density reported in [25], where each lane is 3.7 m wide. All transmitting vehicles apply rank-one precoding based on the strongest eigenmode of the respective links, while the target vehicle applies MMSE receive filtering based on the knowledge of the resulting precoded rank-one channels (both desired and interfering ones). Further, we assume an out of cluster interference of power -10 dB that is neither known nor treated by the target vehicle. For 10000 simulated channel and distance realizations, Fig. 7 shows SINR cumulative distribution function (CDF) plots for increasing values of N . Note that in this setup, $N \geq 7$ is necessary to decode the desired signal interference-free. With $N = 1, 2$, and 4, the system operates in the interference-limited regime and the target vehicle

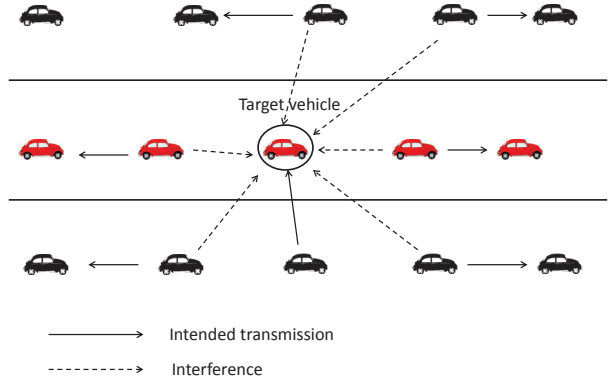


Fig. 6. Three lane highway scenario (figure not drawn to scale).

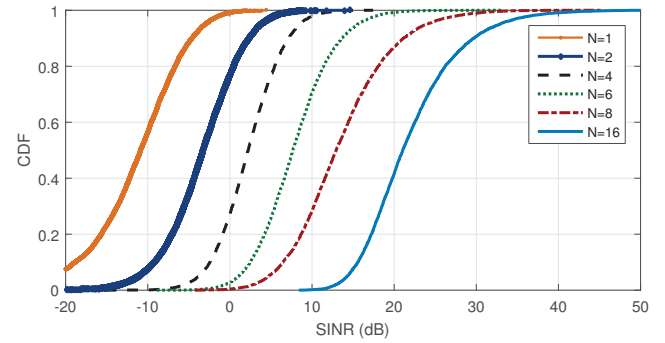


Fig. 7. SINR CDF plots for different number of antennas N .

is heavily affected by interference. As supported by the respective curve, 99%, 77%, and 28% of the SINR values lie below 0 dB in the cases $N = 1, 2$, and 4, respectively. Increasing N to 6 allows canceling all but one interferer, and the resulting SINR improves; nonetheless, 3% of SINR values still lie below 0 dB. For $N = 8$, the target vehicle is able to cancel all interference of neighboring vehicles and the SINR improves as supported by the respective curve. Here, out-of-cluster interference becomes the main system bottleneck (e.g. 10% of SINR values lie below 6.4 dB). However, further increasing N to 16 allows mitigating the effects of the latter due to the increased spatial diversity and MIMO precoding/combining gains, resulting in 99.83% of SINR values above 10 dB.

The main challenge in realizing these promised MIMO gains is to obtain accurate knowledge of the required MIMO channels, which is necessary to perform precoding/receive filtering, with a reasonable pilot overhead. The number of time and/or frequency slots dedicated for pilots necessary to estimate the MIMO channels of active vehicles increases with the number of vehicles and the number of antennas per vehicle. Given that high vehicle mobility results in small coherence times in V2X scenarios, it is thus important to estimate the necessary channels in an efficient way. Reporting of measurements to the base station and control information to the users should also be kept at reasonable levels. Therefore, MIMO techniques can be practical for interference mitigation only for a limited number of nearby users. Investigating new distributed and centralized (e.g. via the base station) user selection algorithms is therefore an important topic for future research.

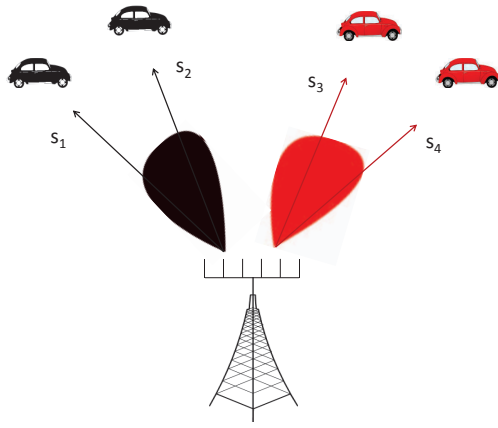


Fig. 8. Hybrid beamforming concept for V2X: "analog" beams radiate power to the directions of vehicular users, while "digital" data precoding can be used to mitigate interference between different users' data streams within each beam.

In practice, a hybrid architecture may be used in V2X scenarios at both ends of the links. On the transmit side, a two-stage procedure first creates "analog" beams to radiate signals into the desired directions and reduce interference to other users. Afterwards, "digital" MIMO schemes are applied on top of beamforming, as shown in Fig. 8. Digital MIMO precoders/receive filters may be adapted on a shorter time scale than analog beams. One advantage of this architecture is that it reduces the dimension of the MIMO channels for digital processing and thus reduces pilot overhead. The hybrid architecture might be especially important in mmWave scenarios to keep good link qualities and also reduce hardware costs. An important topic is how to select beams matched to a vehicle or group of vehicles. Wide beams have less concentrated power to a desired direction and might cause interference in undesired directions, but a narrow beam is very sensitive to high mobility and may need more frequent updating. Some solutions to the problem of beam design can be found in [4], [5]. As shown in the example of Fig. 8, the base station forms two beams, each serving two vehicles. A suitable beam design can mitigate inter-beam interference (e.g. interference between data symbols s_1 and s_3). The remaining interference is intra-beam interference (e.g. interference between data symbol s_1 and s_2), which can be mitigated via well-known digital precoding.

IV. CONCLUSIONS

In this paper, design guidelines were proposed for the physical layer of 5G V2X systems. In the scope of V2X, strengths and weaknesses of existing technologies were discussed, whereas the role of future cellular V2X, including both cmWave and mmWave communication, was highlighted. After elaborating on V2X requirements, with a main focus on latency and reliability, key design aspects for the physical layer were provided, in order to meet these goals. For selected topics of high interest – channel modeling, frame structure, coexistence and synchronization, multi-antenna techniques – preliminary results and solutions were provided, whereas aspects requiring additional study were discussed.

REFERENCES

- [1] V. Jungnickel, K. Manolakis, W. Zirwas, B. Panzner, V. Braun, M. Lossow, M. Sternad, R. Apelfrjd, and T. Svensson, "The role of small cells, coordinated multipoint and massive MIMO in 5G," *IEEE Communications Magazine*, May 2014.
- [2] H. Seo, K.-D. Lee, S. Yasukawa, Y. Peng, and P. Sartori, "Lte evolution for vehicle-to-everything services," *IEEE Communications Magazine*, vol. 54, no. 6, pp. 22–28, 2016.
- [3] 3GPP TR 22.886 V1.0.0: Study on enhancement of 3GPP support for 5G V2X services (Release 15), 3GPP Std., September 2016.
- [4] V. Va, T. Shimizu, G. Bansal, and R. W. H. Jr., "Millimeter wave vehicular communications: A survey," *Foundations and Trends in Networking*, vol. 10, no. 1, pp. 1–113, 2016.
- [5] J. Choi, N. G. Prelcic, R. C. Daniels, C. R. Bhat, and R. W. H. Jr., "Millimeter wave vehicular communication to support massive automotive sensing," *CoRR*, 2016.
- [6] S. Rangan, T. S. Rappaport, and E. Erkip, "Millimeter-wave cellular wireless networks: Potentials and challenges," *Proceedings of the IEEE*, vol. 102, no. 3, pp. 366–385, 2014.
- [7] ETSI TC ITS, "Intelligent Transport Systems (ITS); Vehicular Communications; Basic Set of Applications; Part 2: Specification of Cooperative Awareness Basic Service," Tech. Rep. EN 302 637-2, 2014.
- [8] S.-H. Yu, O. Shih, H.-M. Tsai, N. Wisitpongphan, and R. Roberts, "Smart automotive lighting for vehicle safety," *IEEE Communications Magazine*, vol. 51, no. 12, pp. 50–59, 2013.
- [9] 3GPP TR 22.885 V1.0.0: Study on LTE Support for V2X Services (Release 14), 3GPP Std., September 2015.
- [10] D. S. Baum et al., "IST-2003-507581 WINNER I, D5.4, Final report on link level and system level channel models," Information Society Technologies, Tech. Rep., 2005.
- [11] 3GPP, 3GPP TR 38.900, Channel model for frequency spectrum above 6 GHz, v2.0.0, 3GPP Std., June 2016.
- [12] M. Boban, X. Gong, and W. Xu, "Modeling the evolution of line-of-sight blockage for V2V channels," in *IEEE Vehicular Technology Conference, VTC2016-Fall*, 2016.
- [13] J. Karedal, N. Czink, A. Paier, F. Tufvesson, and A. F. Molisch, "Path loss modeling for vehicle-to-vehicle communications," *IEEE transactions on vehicular technology*, vol. 60, no. 1, pp. 323–328, 2011.
- [14] R. Meireles, M. Boban, P. Steenkiste, O. Tonguz, and J. Barros, "Experimental study on the impact of vehicular obstructions in vanets," in *IEEE Vehicular Networking Conference (VNC)*, Dec. 2010, pp. 338–345.
- [15] M. Boban, J. Barros, and O. Tonguz, "Geometry-based vehicle-to-vehicle channel modeling for large-scale simulation," *IEEE Transactions on Vehicular Technology*, vol. PP, no. 99, pp. 1–1, 2014.
- [16] T. Abbas, K. Sjöberg, J. Karedal, and F. Tufvesson, "A measurement based shadow fading model for vehicle-to-vehicle network simulations," *International Journal of Antennas and Propagation*, vol. 2015, 2015.
- [17] J. Karedal, F. Tufvesson, N. Czink, A. Paier, C. Dumard, T. Zemen, C. Mecklenbrauker, and A. Molisch, "A geometry-based stochastic mimo model for vehicle-to-vehicle communications," *Wireless Communications, IEEE Transactions on*, vol. 8, no. 7, pp. 3646–3657, July 2009.
- [18] J. Maurer, T. Fugen, T. Schafer, and W. Wiesbeck, "A new inter-vehicle communications (ivc) channel model," in *IEEE Vehicular Technology Conference, VTC2004-Fall*, vol. 1, IEEE, 2004, pp. 9–13.
- [19] G. Acosta-Marum and M. Ingram, "Six time- and frequency- selective empirical channel models for vehicular wireless lans," *IEEE Vehicular Technology Magazine*, vol. 2, no. 4, pp. 4–11, dec. 2007.
- [20] K. Manolakis and W. Xu, "Time synchronization for multi-link D2D/V2X communication," in *IEEE 84th Vehicular Technology Conference (VTC)*, 2016.
- [21] TS36.211, V13.1.0: Technical Specification Group Radio Access Network; Evolved Universal Terrestrial Radio Access (E-UTRA); Physical channels and modulation (Release 13), 3GPP Std., 2016.
- [22] E. Lahetkangas, K. Pajukoski, E. Tiirola, G. Berardinelli, I. Harjula, and J. Vihriala, "On the TDD subframe structure for beyond 4G radio access network," in *Future Network and Mobile Summit (FutureNetworkSummit)*, 2013, July 2013, pp. 1–10.
- [23] 3GPP, Report of 3GPP TSG RAN WG1 86 v0.2.0, 3GPP Std., August 2016.
- [24] M. Ibrahim and W. Xu, "A comparison of symbol-wise and self-contained frame structure for 5g services," in *2016 IEEE Globecom Workshops (GC Wkshps)*, Dec 2016.
- [25] N. Wisitpongphan, F. Bai, P. Mudalige, V. Sadekar, and O. Tonguz, "Routing in Sparse Vehicular Ad Hoc Wireless Networks," *IEEE Journal on Selected Areas in Communications*, vol. 25, no. 8, pp. 1538–1556, Oct. 2007.